



**BNL-93880-2010-BC**

***Nonlinear dynamics experiments***

**W. Fischer**

*To be published in "Handbook of Accelerator Physics and Engineering"*

July 2010

**Collider-Accelerator Department**

**Brookhaven National Laboratory**

P.O. Box 5000

Upton, NY 11973-5000

[www.bnl.gov](http://www.bnl.gov)

Notice: This manuscript has been authored by employees of Brookhaven Science Associates, LLC under Contract No. DE-AC02-98CH10886 with the U.S. Department of Energy. The publisher by accepting the manuscript for publication acknowledges that the United States Government retains a non-exclusive, paid-up, irrevocable, world-wide license to publish or reproduce the published form of this manuscript, or allow others to do so, for United States Government purposes.

This preprint is intended for publication in a journal or proceedings. Since changes may be made before publication, it may not be cited or reproduced without the author's permission.

## **DISCLAIMER**

This report was prepared as an account of work sponsored by an agency of the United States Government. Neither the United States Government nor any agency thereof, nor any of their employees, nor any of their contractors, subcontractors, or their employees, makes any warranty, express or implied, or assumes any legal liability or responsibility for the accuracy, completeness, or any third party's use or the results of such use of any information, apparatus, product, or process disclosed, or represents that its use would not infringe privately owned rights. Reference herein to any specific commercial product, process, or service by trade name, trademark, manufacturer, or otherwise, does not necessarily constitute or imply its endorsement, recommendation, or favoring by the United States Government or any agency thereof or its contractors or subcontractors. The views and opinions of authors expressed herein do not necessarily state or reflect those of the United States Government or any agency thereof.



### 0.0.1 Nonlinear Dynamics Experiments

*W. Fischer, BNL*

The goal of nonlinear dynamics experiments is to improve the understanding of single particle effects that increase the particle amplitude and lead to loss. Particle motion in storage rings is nearly conservative and for transverse dynamics the Hamiltonian in action angle variables  $(I_x, I_y, \phi_x, \phi_y)$  near an isolated resonance  $k\nu_x + l\nu_y \approx p$  is

$$H = I_x\nu_{x0} + I_y\nu_{y0} + g(I_x, I_y) + h(I_x, I_y) \cos(k\phi_x + l\phi_y - p\theta), \quad (1)$$

where  $k, l, p$  are integers,  $\theta = 2\pi s/L$  is the azimuth, and  $s$  and  $L$  are the path length and circumference respectively. The amplitude dependent tunes are given by

$$\nu_{x,y}(I_x, I_y) = \nu_{x0,y0} + \partial g(I_x, I_y)/\partial I_{x,y} \quad (2)$$

and  $h(I_x, I_y)$  is the resonance driving term (RDT). If the motion is governed by multiple resonances,  $h(I_x, I_y)$  has to be replaced by a series of terms. The particle motion is completely determined by the terms  $g$  and  $h$ , which can be calculated from higher order multipoles (Sec. ??), or obtained from simulations. Deviations from pure Hamiltonian motion occur due to synchrotron radiation damping (Sec. ??) in lepton or very high energy hadron rings, parameter variations, and diffusion processes such as residual gas and intrabeam scattering. The time scale of the non-Hamiltonian process determines the applicability of the Hamiltonian analysis.

Transverse nonlinearities are introduced through sextupoles or higher order multipoles and magnetic field errors in dipoles and quadrupoles. Sextupoles can already drive all resonances. The beam-beam interaction and space charge also introduce nonlinear fields.

Intentionally introduced nonlinearities are used to extract beam on a resonance or through capture in stable islands [1]. Localization and minimization of nonlinearities in a ring is a general strategy to decrease emittance growth and increase the beam lifetime. The minimization of nonlinear effects can be done locally or globally. Except for resonant extraction, amplitude increase and particle loss is the result of chaotic particle motion. Large chaotic regions allow particles to increase their amplitudes, and ensures their ultimate loss. However, chaotic particles can, on average, still survive the time period of interest, i.e. the storage time.

Nonlinear dynamics experiments aim to determine either the detuning and driving terms  $g$  and  $h$  directly, or their effect on other quantities. Nonlinear phenomena observed in experiments include phase space deformations and resonant islands in Poincaré surfaces of section, nonlinear phase advances, amplitude detuning  $g$ , decoherence (Sec. ??), resonance driving terms  $h$ , smear, halo formation, echoes (Sec. ??), the tune response matrix [2], dynamic aperture (Sec. ??), emittance growth, and particle loss. Nonlinear experiments can also be done in the longitudinal plane [3].

**Surface of section** The properties of a nonlinear Hamiltonian system can be visualized by a Poincaré surface of section, where the phase space variables of the particle trajectory are plotted turn-by-turn (TBT). This is the experimental determination of the 1-turn map. It reveals distortions of trajectories and resonant islands. Photographs of synchrotron light from as early as 1968 show beam trapped in transverse resonance islands [4]. The surface of section can be reconstructed from two TBT readings of a pair of Beam Position Monitors (BPMs), where the ideal phase advance between the 2 BPMs is an odd multiple of  $\pi/2$ . For Fig. 1 a 45 MeV proton beam was cooled in the IUCF and kicked to different horizontal amplitudes [5].

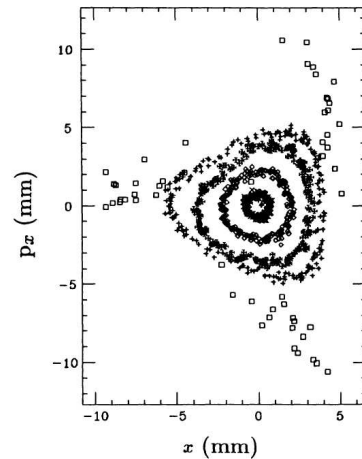


Figure 1: Experimental Poincaré surface of section near a third integer resonance obtained from BPM data after kicking the beam to different betatron amplitudes in the IUCF (reprinted with permission from [5], copyright by APS).

**Detuning and RDTs** A Hamiltonian system is completely characterized by the amplitude dependent tune shift, and the resonance driving terms

(Sec. ??). To measure the amplitude detuning, the beam is kicked to different amplitudes and the tune obtained from a spectral analysis of the TBT data [5–8]. The tune error  $\Delta\nu$  in a Fast Fourier Transformation (FFT) is proportional to  $1/N$ , where  $N$  is the number of turns used, and can be improved to be proportional to  $1/N^4$  [9, 10]. Figure 2 shows a detuning measurement in VEPP-4M, where a 1.8 GeV electron beam was kicked and observed in BPMs for up to 4096 turns [6].

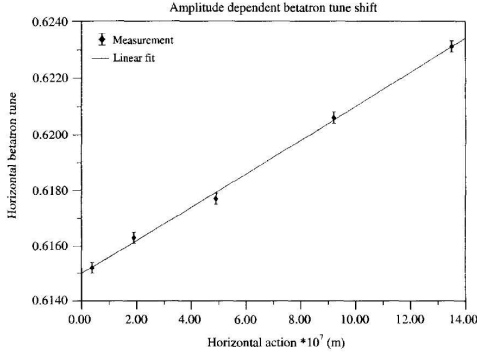


Figure 2: Typical amplitude dependence of betatron tune measured in VEPP-4M (courtesy V. Sajaev).

Resonance driving terms can also be derived from turn-by-turn BPM data (Fig. 3). With an ac dipole a coherent dipole motion of indefinite length can be induced [11] and thereby the signal-to-noise ratio increased compared to kick-based measurement [7]. The length of the turn-by-turn measurement is then limited by the BPM system.

With the reliable measurement of  $s$ -dependent changes in resonance driving terms, multipole fields can be inferred and the correction of single or multiple resonances becomes possible [12].

**Tune and amplitude diffusion** Mapping the frequencies (tunes) as a function of initial conditions  $(I_x, I_y)$  is often referred to as Frequency Map Analysis (FMA) [9]. Precise tune measurements [9, 10] allow the experimental determination of frequency maps that reveal potentially harmful resonances (Fig. 4). Also accessible is the tune change over time  $\Delta\nu = \nu(T_1) - \nu(T_2)$ , where  $T_1$  and  $T_2$  are consecutive intervals, which is a measure of the tune diffusion.

The time evolution of a particle distribution  $f(I, t)$  with amplitude diffusion is given by [13]

$$\frac{\partial}{\partial t} f(I, t) = \frac{\partial}{\partial I} D(I) \frac{\partial}{\partial J} f(I, t) \quad (3)$$

where  $D(I) = \langle \Delta I^2 \rangle / (2\Delta t)$  is the amplitude dependent diffusion coefficient. Over small ampli-

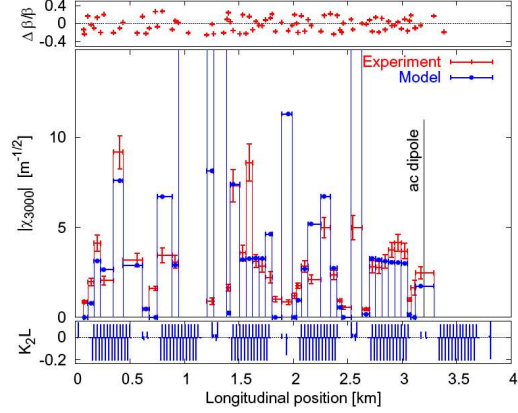


Figure 3: Measurement of sextupolar local term  $|\chi_{3000}|$  in RHIC with an ac dipole. This term is proportional to a driving term  $h$  for the resonance  $3\nu_x = p$ . The bottom plot shows the sextupolar components in the ring (reprinted with permission from [7], copyright by APS).

tude ranges, such as those created when a scraper is moved from position  $I_c$ ,  $D(I)$  can be assumed constant and the change in the loss rate at the scraper can be fitted to obtain  $R = D(I_c)/I_c^2$  (Fig. 5). Larger regions of  $I$  are sampled when the time evolution of the transverse profiles are recorded. To access large amplitudes the beam is kicked, often creating a hollow beam [8, 15]. Diffusion rates, caused by a number of mechanisms, can span many orders of magnitudes [16].

**Dynamic aperture and tune modulation** The dynamic aperture (DA) determined in simulations is displayed as survival plots (Sec. ??). In an experiment a single large kick places a large number of particles across the DA. The DA is then determined as the maximum amplitude where particles can be observed with a transverse profile monitor, for example with a wire scanner (Fig. 6). Increasing the emittance with many small kicks is also possible but requires a higher sensitivity in the transverse profile monitor. In lepton machines, where the survival times of particles only need to be of the same order as the synchrotron radiation damping time, the beam is usually kicked until beam loss is observed.

Tune modulation is caused by the synchrotron motion and non-zero chromaticity as well as power supply ripples in the quadrupoles. Tune modulation affects the long-term stability of particle motion. In the presences of an isolated resonance with island tune  $\nu_I$ , the modulated tune

$$\nu(N) = \nu_0 + q \sin(2\pi\nu_M N), \quad (4)$$

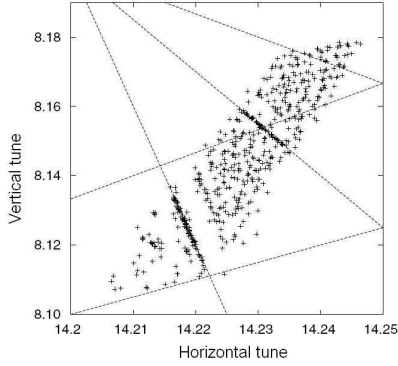


Figure 4: Experimental frequency map for the ALS. At a fixed set tune the beam is kicked to different amplitudes and the beam oscillation frequency is obtained from turn-by-turn BPM data. The dotted lines are resonances of order  $\leq 5$  (reprinted with permission from [14], copyright by APS).

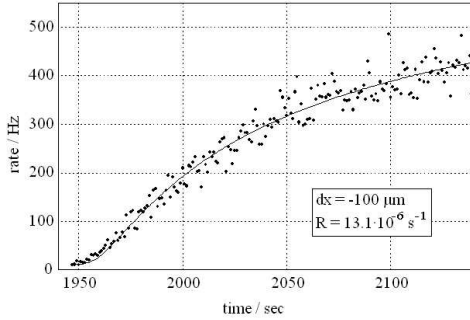


Figure 5: Particle loss rate at a HERAp collimator after retraction by  $100 \mu\text{m}$ , fitted time-dependent loss curve and diffusion constant  $R$  (courtesy M. Seidel [17]).

where  $N$  is the turn number, and  $q$  and  $\nu_M$  are the modulation depth and tune, leads to four different phases in the  $(\nu_M/\nu_I, q/\nu_I)$  diagram (Fig. 7). Massive chaos occurs when sidebands created by the modulation overlap (Chirikov criterion [18]). Tune modulation effects have been studied extensively [8, 19, 20].

## References

- [1] R. Cappi, M. Giovannozzi, PRST-AB **7**, 024001 (2004); M. Giovannozzi et al., PRST-AB **12**, 024003 (2009)
- [2] G. Franchetti, A. Parfenova, and I. Hofmann, PRST-AB **11**, 094001 (2008).
- [3] M. Ellison et al., PRL **70**, 591 (1993).
- [4] G.N. Kulipanov et al., Novosibirsk Preprint INP 68-251 (1968)
- [5] D.D. Caussyn et al., PR A **46**, 7942 (1992)
- [6] V. Kiselev et al., PA **57**, 65 (1997)
- [7] R. Tomás et al., PRST-AB **8**, 024001 (2005)

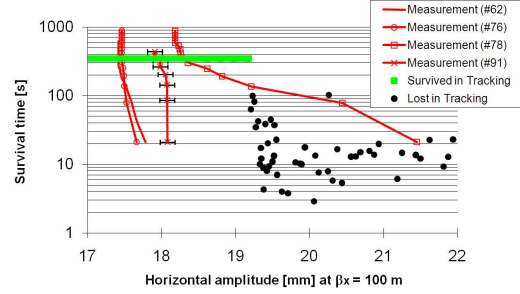


Figure 6: Measured and simulated DA in SPS with 8 strong sextupoles and tune modulation with parameters  $q = 1.87 \times 10^{-3}$  and  $\nu_M = 2.1 \times 10^{-4}$  (reprinted with permission from [8], copyright by APS).

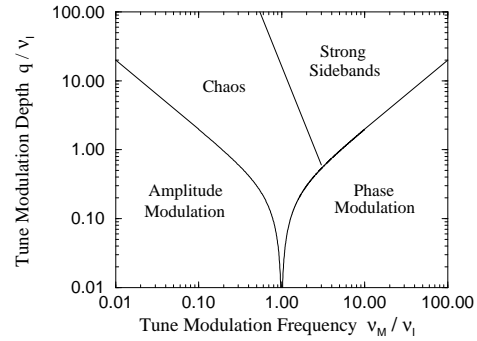


Figure 7: Approximate boundaries between dynamical phases in tune modulation space (reprinted with permission from [19], copyright by APS).

- [8] W. Fischer, M. Giovannozzi, F. Schmidt, PR E **55**, 3507 (1997)
- [9] H.S. Dumas and J. Laskar, Phys. Rev. Lett. **70**, 2975 (1993)
- [10] R. Bartolini et al., PA **52**, 147 (1996)
- [11] M. Bai et al., PR E56, 6002 (1997)
- [12] R. Bartolini et al., PRST-AB **11**, 104002 (2008)
- [13] K.-H. Mess, M. Seidel, NIM A **351**, 279 (1994)
- [14] D. Robin et al., PRL **85**, 558 (2000)
- [15] T. Chen et al. PRL **68**, 33 (1992)
- [16] F. Zimmermann, PA **49**, 67 (1995)
- [17] M. Seidel, Ph.D. thesis, Hamburg U., DESY 94-103 (1994).
- [18] B.V. Chirikov, Physics Report **52**, 263 (1979)
- [19] T. Satogata et al., PRL **68**, 1838 (1992)
- [20] O.S. Brüning, F. Willeke, PA **55**, 237 (1996)